



ELSEVIER

Contents lists available at ScienceDirect

## Ultramicroscopy

journal homepage: [www.elsevier.com/locate/ultramic](http://www.elsevier.com/locate/ultramic)

## Patterning pentacene surfaces by local oxidation nanolithography

N.S. Losilla<sup>a,\*</sup>, J. Martinez<sup>a</sup>, E. Bystrenova<sup>b</sup>, P. Greco<sup>b</sup>, F. Biscarini<sup>b</sup>, R. García<sup>a,\*</sup><sup>a</sup> Instituto de Microelectrónica de Madrid: CSIC, Isaac Newton 8, 28760 Tres Cantos, Madrid, Spain<sup>b</sup> Institute for Nanostructured Materials: CNR (ISMN-CNR), Via Gobetti 101, 40129 Bologna, Italy

## ARTICLE INFO

## Keywords:

Organic semiconductor  
Pentacene  
AFM nanolithography  
Local oxidation  
Nanolithography  
Tip-based nanofabrication

## ABSTRACT

Sequential and parallel local oxidation nanolithographies have been applied to pattern pentacene samples by creating a variety of nanostructures. The sequential local oxidation process is performed with an atomic force microscope and requires the application of a sequence of voltage pulses of 36 V for 1 ms. The parallel local oxidation process is performed by using a conductive and patterned stamp. Then, a voltage pulse is applied between the stamp and the pentacene surface. Patterns formed by arrays of parallel lines covering 1 mm<sup>2</sup> regions and with a periodicity of less than 1 μm have been generated in a few seconds. We also show that the patterns can be used as templates for the deposition of antibodies.

© 2010 Elsevier B.V. All rights reserved.

## 1. Introduction

Organic semiconductors have emerged as attractive materials for the fabrication of low cost and flexible electronic devices. Organic semiconductors are being used as active elements in electronic devices such as organic light-emitting diodes (OLED) [1], thin film transistors (TFT) [2–7], organic solar cells [8], organic field-effect transistors (OFET) [9], electrochemical transistors, and recently in biosensing applications [10–12]. In the field of organic semiconductor research, pentacene is one of the most studied materials, thanks to its high mobility comparable with that of amorphous silicon devices [13]. High-performance electronic devices are easily and robustly obtained from vacuum-deposited thin films of pentacene on a variety of substrates. In the present work, monolayers of pentacene were evaporated on Si (100) substrates and then nanopatterned by local oxidation nanolithography.

Local oxidation nanolithography performed with an atomic force microscope (AFM) has established itself as a robust, reliable, and flexible method to pattern a variety of materials such as semiconductor, metallic, and organic surfaces [14–20]. In the oxidation process, the AFM tip acts as a cathode and the water meniscus formed between tip and surface is the source for the oxyanions species [21,22]. The strong localization of the electrical field lines near the tip apex and the lateral confinement of the oxyanions species within the liquid meniscus give rise to a nanometer-size structure.

Here, we also show that local oxidation on pentacene can be upscaled by using a print-based approach.

By following soft lithography and nanoimprint methods [23,24], several authors have upscaled the local oxidation process by using a conductive stamp with multiple protrusions as a cathode. Mühl et al. [25] used a stamp with a few protrusions. Cavallini et al. [26] used as a stamp a digital videodisk (DVD) sample and transferred its bits to a silicon surface. Martinez et al. [27,15] used silicon stamps made by electron beam lithography to generate arrays of parallel lines separated by 100 nm over mm<sup>2</sup> regions. Sagiv et al. used as a stamp a transmission electron microscopy grid to oxidize self-assembled monolayers [28–30]. In the present work, we replicated the motives of the stamp used in the experiments on organic semiconductor substrates.

Here, we show that pentacene samples can be locally oxidized with the AFM and a parallel oxidation instrument. In this way, different nanostructures have been created on top of pentacene islands. We also show that the pentacene nanopatterns can be used as a template for controlling the adsorption of biological molecules.

## 2. Experimental methods

## 2.1. Atomic force microscopy (AFM)

Amplitude modulation AFM imaging (AM-AFM) and nanolithography was performed using a Dimension V Scanning Probe Microscope (Veeco Instruments, USA) with *n*(+)-silicon cantilevers (Nano World, resistivity ~0.01–0.0025 Ω cm, spring constant ~ 42 N m<sup>-1</sup>). Amplitude modulation AFM images were recorded with NanoScope V controller operated in noncontact mode. Local oxidation nanolithography and imaging were performed using a 100 μm Hybrid XYZ scanner. This scanner

\* Corresponding authors.

E-mail addresses: [nuria@imm.cnm.csic.es](mailto:nuria@imm.cnm.csic.es) (N.S. Losilla), [rgarcia@imm.cnm.csic.es](mailto:rgarcia@imm.cnm.csic.es) (R. García).

provides accurate control of the in-plane position and movement of the AFM probe to obtain high-definition nanolithography.

## 2.2. Parallel local oxidation set-up

Parallel local oxidation was performed using a home-made instrument which enables to pattern nanoscale motives over  $1\text{ cm}^2$  regions [27]. The sample is approached towards the stamp with submicrometer accuracy. The sample base can pivot with respect to three fixed points. Submicrometer approach together with pivotal rotation allows to compensate an increase of the local pressure in a region of the sample.

## 2.3. Stamp fabrication

The polydimethylsiloxane (PDMS) stamps (Sylgard 184 Silicone Elastomer) were prepared by replica molding [31] using, as a master, the surface of a commercial digital versatile disc (DVD), composed of an array of parallel lines with a periodicity of 760 nm, full width at half maximum (FWHM) 350 nm and a height of 100 nm. After the curing process, carried out for 1 h at  $90\text{ }^\circ\text{C}$ , the replica is peeled off from the master and washed in absolute ethanol to clean the surface. Finally, the surface of the PDMS stamp was coated with a double-layer of metals by electron beam evaporation (5 nm Cr and 60 nm Au).

## 2.4. Pentacene growth

Pentacene (Sigma Aldrich Oekanal, Analytical Standard) was grown by high vacuum sublimation on a silicon (1 0 0) surface covered with a very thin native silicon oxide film. Base pressure in the evaporation chamber was  $8 \times 10^{-7}$  mbar. The evaporation rates of  $10\text{ \AA}/\text{min}$  and substrate temperature (298 K) were chosen to obtain layered structures.

## 2.5. Antibodies

Pentacene samples modified by parallel local oxidation were incubated with monoclonal anti-bovine serum albumin (anti-BSA) (B 2901, Sigma) solution ( $1\text{ }\mu\text{g}/\text{ml}$  in deionized water (DI water) solution) for 30 s and subsequently rinsed with DI water and blow dry in  $\text{N}_2$ .

## 3. Results

The goal is to nanopattern pentacene surfaces. For that purpose we have used two different albeit complementary approaches: Local oxidation nanolithography (LON) by atomic force microscopy (AFM) and parallel local oxidation using a home-built imprinting instrument.

Fig. 1(a) shows an overview of AFM local oxidation process. A water meniscus provides both the chemical species (oxyanions)

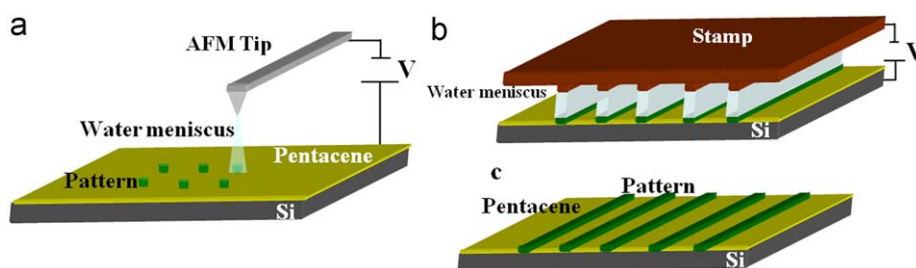


**Fig. 1.** (a) AFM local oxidation scheme. A voltage pulse applied between the AFM tip and the surface yields to the formation of a water meniscus. This meniscus confines an anodic oxidation reaction allowing the modification a pentacene surface. (b) Schematics of the set-up for performing the local oxidation lithography in parallel. The contact between the stamp and the substrate provides the water menisci that are involved in the mechanisms of the modification of pentacene layers. (c) Scheme of the sample after being patterned by parallel local oxidation.

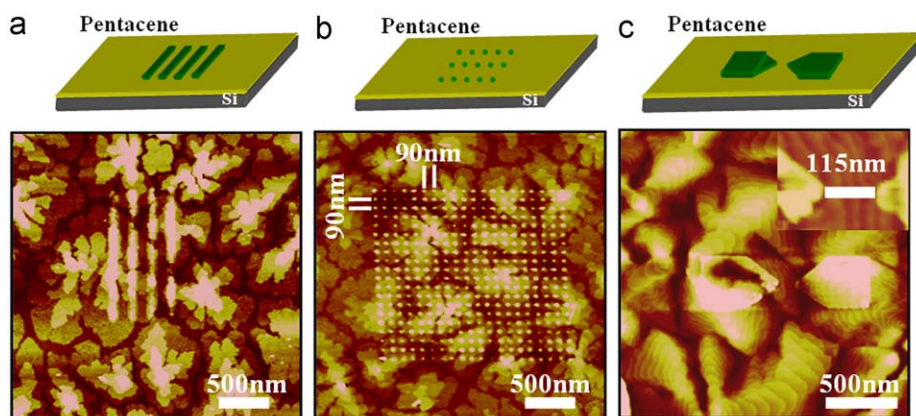


**Fig. 2.** Schemes and amplitude modulation AFM images of different patterns on pentacene: (a) Pentacene pattern formed by four stripes with a separation of 200 nm. (b) A periodic array of 90 nm dots. (c) Pentacene patterns with a gap separation of about 115 nm on top of 20 ML of pentacene.

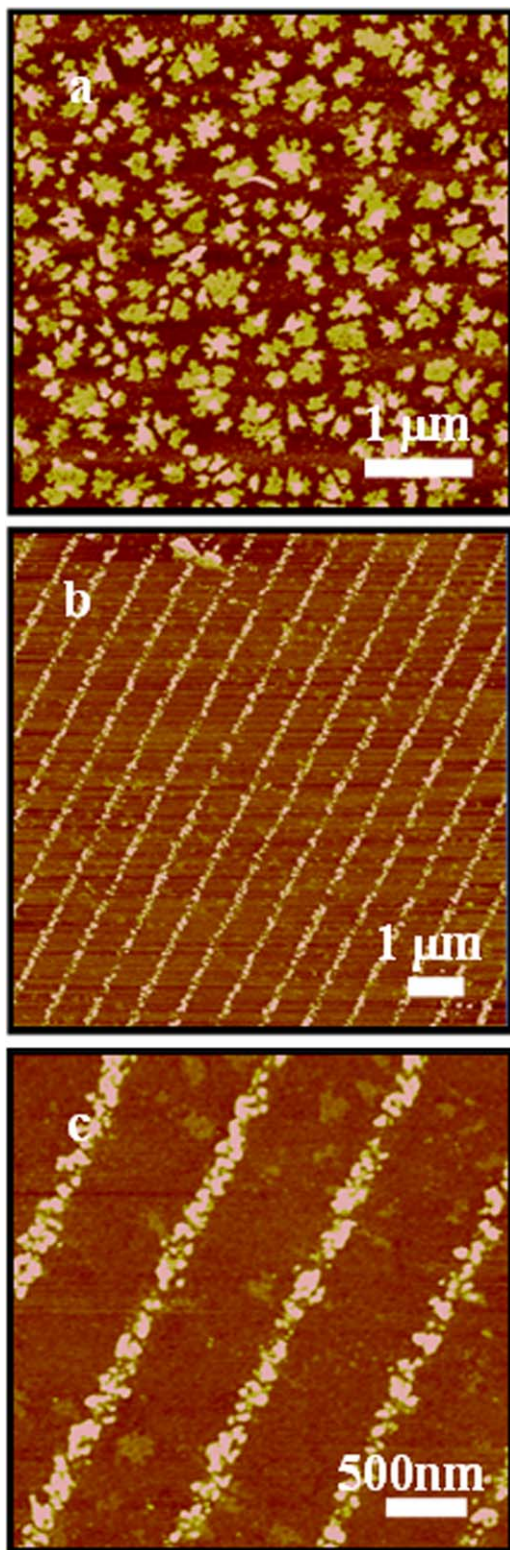


**Fig. 3.** (a) Amplitude modulation AFM image of several monolayers of pentacene evaporated on a silicon substrate before the nanolithography. (b, c) AM-AFM topographic images of patterns fabricated by parallel local oxidation nanolithography. The stripes are 150 nm wide and are separated by 600 nm.

and the spatial confinement for the anodic oxidation of a nanometer-size region of the sample surface. The application of a voltage pulse between the tip and the sample polarizes the

water molecules in the vapor phase and those absorbed on the sample surface. When the voltage is above a certain threshold value, a field-induced liquid meniscus is formed between the tip and the sample surface. The AFM tip acts as a cathode and the water meniscus provides the oxyanions. Furthermore, local oxidation is amenable to parallel processing by replacing the AFM tip by a stamp with thousand of reliefs. A scheme of the process is presented in Fig. 1(b). Parallel local oxidation enables nanopatterning of large areas in a few seconds as it is shown in Fig. 1(c).

First, the pentacene islands were patterned by AFM local oxidation. For that purpose, pentacene monolayers were deposited by thermal sublimation on top of Si(1 0 0) surfaces. The growth conditions were adjusted to obtain pentacene samples of different thicknesses. In this way, different patterns have been created by applying a sequence of voltage pulses with an amplitude of 36 V and a duration of 1 ms between the AFM tip and the pentacene. The nanopatterning experiments were performed at room temperature. Fig. 2(a) shows a pattern formed by four stripes with a separation of 200 nm. By optimizing the nanolithography parameters, it was possible to fabricate an array of dots with a periodicity of 90 nm on top of the pentacene islands as shown in Fig. 2(b). These images (Figs. 2(a) and (b)) show a morphology characterized by the presence of islands formed by four monolayers (ML) of pentacene. Most of the islands show a dendritic shape.

Fig. 2(c) shows a pattern made of two pointed arrows separated above 115 nm on top of 20 ML of pentacene on silicon.

The successful patterning of pentacene by AFM nanolithography has motivated us to perform experiments to modify large areas of pentacene. To achieve that, we have applied parallel local oxidation experiments, where the cathode is a stamp with multiple protrusions. In these experiments, the stamp and the sample were introduced in the home-made instrument described in the parallel local oxidation set-up section, and connected to a power supply. When a bias voltage of 36 V is applied between the stamp and the substrate for 1 min, a replica of the stamp's pattern is formed on the pentacene surface. Stripes with same periodicity of the stamp appear on top of the pentacene islands (Figs. 3(b) and (c)). The stripes were 150 nm wide and separated by 600 nm.

The patterned pentacene surfaces have been used to direct the deposition of antibodies. For this, anti-BSA molecules were drop casted on the patterned pentacene templates. Previous topography and recognition experiments have demonstrated that single antibodies remained fully functional after deposition on the organic semiconductor pentacene [32]. A 40 μl drop of a 1 μg/ml solution containing anti-BSA was deposited on the pentacene patterned samples for 30 s. The sample was then rinsed in DI water and blown dry in N<sub>2</sub>. The AFM images (Figs. 4(b) and (c)) show significant differences with respect to the surface prior to deposition (Figs. 3(b) and (c)). We observe that aggregates of anti-BSA molecules bind preferentially to the pentacene lines.

#### 4. Conclusions

We show that AFM and parallel local oxidation can be used to fabricate different nanopatterns on pentacene surfaces. The patterned features exhibit periodicities below 100 nm. For example, we have fabricated a matrix of 20 dots with a lattice parameter of 90 nm. We demonstrate that the patterned pentacene templates can be used for a controlled deposition of anti-BSA antibodies.

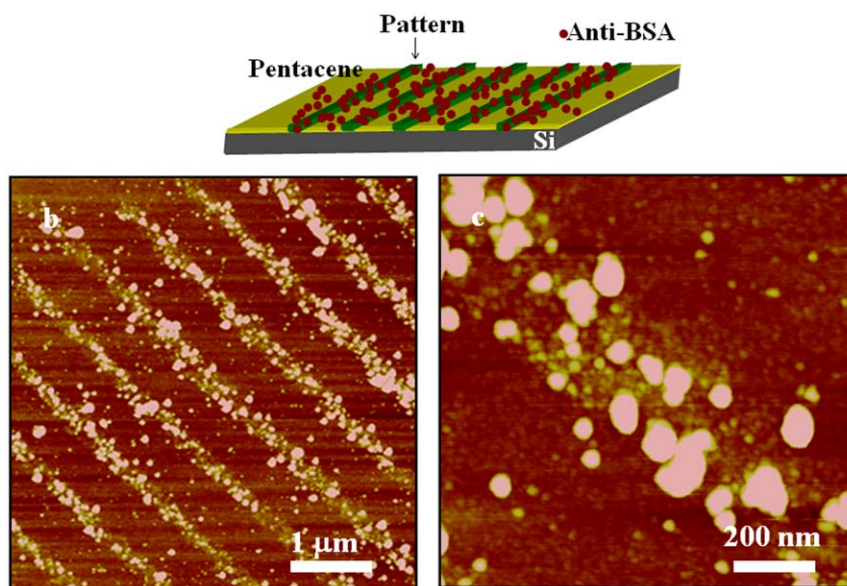


**Fig. 4.** (b) Scheme of the directed deposition of antibodies on pentacene surfaces. (b, c) AM-AFM images of anti-BSA molecules deposited on the pentacene surfaces shown in Figs. 3(a) and (c).

#### Acknowledgments

This work was financially supported by the Ministerio de Educación y Ciencia (MAT2006-03833,) the CSIC (PIF2008, TRANSBIO), and the European Commission (BIODOT,NMP4-CT-2006-032652).

#### References

- [1] A.P. Kulkarni, C.J. Tonzola, A. Babel, S.A. Jenekhe, *Chem. Mater.* 16 (2004) 4556–4573.
- [2] C. Reese, Z. Bao, *Mater. Today* 10 (2007) 20–27.
- [3] O.D. Jurchescu, J. Baas, T.T.M. Palstra, *Appl. Phys. Lett.* 84 (2004) 3061–3063.
- [4] A. Facchetti, M. Muehlebach, M.H. Yoon, G.R. Hutchison, M.A. Ratner, T.J. Marks, *J. Am. Chem. Soc.* 126 (2004) 13480–13501.
- [5] G.H. Gelinck, H.E.A. Huitema, E. Van Veenendaal, E. Cantatore, L. Schrijnemakers, J.B.P.H. Van der Putten, T.C.T. Geuns, M. Beenhakkers, J.B. Giesbers, B.H. Huisman, E.J. Meijer, E.M. Benito, F.J. Touwslager, A.W. Marsman, B.J.E. Van Rens, D.M. De Leeuw, *Nat. Mater.* 3 (2004) 106–110.
- [6] L.B. Roberson, J. Kowalik, L.M. Tolbert, C. Kloc, R. Zeis, X. Chi, R. Fleming, C. Wilkins, *J. Am. Chem. Soc.* 127 (2005) 3069–3075.
- [7] P.T. Herwig, K.A. Mullen, *Adv. Mater.* 11 (1999) 480–483.
- [8] P. Peumans, A. Yakimov, S.R. Forrest, *J. Appl. Phys.* 93 (2003) 3693–3723.
- [9] G. Horowitz, P. Lang, M. Mottaghi, H. Aubin, *Adv. Funct. Mater.* 14 (2004) 1069–1074.
- [10] Y. Cui, Q. Wei, H. Park, C.M. Lieber, *Science* 293 (2001) 1289–1292.
- [11] F. Patolsky, B.P. Timko, G.F. Zheng, C.M. Lieber, *MRS Bull.* 32 (2007) 142–149.
- [12] E. Stern, J.F. Klemic, D.A. Routenberg, P.N. Wyrembak, D.B. Turner-Evans, A.D. Hamilton, D.A. LaVan, T.M. Fahmy, M.A. Reed, *Nature* 445 (2007) 519–522.
- [13] D.J. Gundlach, Y.Y. Lin, T.N. Jackson, S.F. Nelson, D.G. Schlom, *IEEE Electron Device Lett.* 18 (1997) 87–89.
- [14] R.V. Martinez, N.S. Losilla, J. Martinez, Y. Huttel, R. Garcia, *Nano Lett.* 7 (2007) 1846–1850.
- [15] R.V. Martinez, N.S. Losilla, J. Martinez, M. Tello, R. Garcia, *Nanotechnology* 18 (2007) 084021–084027.
- [16] R. Garcia, R.V. Martinez, J. Martinez, *Chem. Soc. Rev.* 35 (2006) 29–38.
- [17] L. Pellegrino, I. Pallecchi, D. Marre, E. Bellingeri, A.S. Siri, *Appl. Phys. Lett.* 81 (2002) 3849–3851.
- [18] N. Clement, A. Francinelli, D. Tonneau, Ph. Scotto, F. Jandard, H. Dallaporta V. Safarov, D. Fraboulet, J. Gautier, *Appl. Phys. Lett.* 82 (2003) 1727–1729.
- [19] R. Crook, A.C. Graham, C.G. Smith, I. Farrer, H.E. Beere, D.A. Ritchie, *Nature* 424 (2003) 751–754.
- [20] C.F. Chen, S.D.T. Zeng, H.Y. Chen, S. Gwo, *Opt. Lett.* 30 (2005) 652–654.
- [21] M. Calleja, J. Anguita, R. Garcia, K. Birkelund, F. Perez-Murano, J.A. Dagata, *Nanotechnology* 10 (1999) 34–38.
- [22] H. Kuramochi, K. Ando, T. Tokiza, H. Yokohama, *Appl. Phys. Lett.* 84 (2004) 4005–4014.
- [23] H.O. Jacobs, G.M. Whitesides, *Science* 291 (2001) 1763–1766.
- [24] P.F. Murphy, K.J. Morton, Z.L. Fu, S.Y. Chou, *Appl. Phys. Lett.* 90 (2007) 203115–203122.
- [25] T. Mühl, J. Kretz, I. Mönch, C.M. Schneider, H. Brückl, G. Reiss, *Appl. Phys. Lett.* 76 (2000) 786–788.
- [26] M. Cavallini, P. Mei, F. Biscarini, R. Garcia, *Appl. Phys. Lett.* 83 (2003) 5286–5288.
- [27] J. Martinez, N.S. Losilla, F. Biscarini, G. Schmidt, T. Borzenko, L.W. Molenkamp, R. Garcia, *Rev. Sci. Instrum.* 77 (2006) 086106–086111.
- [28] S. Hoeppeener, R. Maoz, J. Sagiv, *Nano Lett.* 3 (2003) 761–767.
- [29] S. Liu, R. Maoz, J. Sagiv, *Nano Lett.* 4 (2004) 845–851.
- [30] A. Zeira, D. Chowdhury, R. Maoz, J. Sagiv, *ACS Nano* 2 (2008) 2554–2558.
- [31] M. Cavallini, P. Stolar, J.F. Moulin, M. Surin, P. Leclère, R. Lazzaroni, D. Werner Breiby, J.W. Andreasen, M.M. Nielsen, P. Sonar, A.C. Grimdale, K. Müllen, F. Biscarini, *Nano Lett.* 5 (2005) 2422–2425.
- [32] J. Preiner, N.S. Losilla, A. Ebner, P. Annibale, F. Biscarini, R. Garcia, P. Hinterdorfer, *Nano Lett.* 9 (2009) 571–575.